

The Diffusion Tensor Imaging Features in the Visual Pathways of Patients with Cavernous Sinus Meningioma Treated by Gamma Knife Radiosurgery

Hafize Otçu Temur¹, Alpay Alkan¹, Mustafa Aziz Hatiboğlu², İsmail Yurtsever¹, Kerime Akdur², Özlem Toluk³, Mehmet Hakan Seyithanoğlu²

¹Department of Radiology, Bezmialem Vakıf University Faculty of Medicine, İstanbul, Türkiye

²Department of Neurosurgery, Bezmialem Vakıf University Faculty of Medicine, İstanbul, Türkiye

³Department of Biostatistics, Bezmialem Vakıf University Faculty of Medicine, İstanbul, Türkiye

Cite this article as: Otçu Temur H, Alkan A, Hatiboğlu MA, et al. The diffusion tensor imaging features in the visual pathways of patients with cavernous sinus meningioma treated by gamma knife radiosurgery. *Current Research in MRI*, 2025;4(1):7-11.

Corresponding author: Hafize Otçu Temur, e-mail: hotcutemur@bezmialem.edu.tr

Received: March 27, 2025 **Revision Requested:** April 24, 2025 **Last Revision Received:** May 28, 2025 **Accepted:** June 17, 2025 **Publication Date:** August 22, 2025

DOI: 10.5152/CurrResMRI.2025.25113



Content of this journal is licensed under a Creative Commons Attribution-NonCommercial 4.0 International License.

Abstract

Objective: The objectives of this study are to evaluate the effects of diffusion tensor imaging (DTI) on visual pathways following Gamma Knife radiosurgery (GKR) and to identify any correlations between DTI results and radiosurgery data.

Methods: Thirteen patients with cavernous sinus meningiomas (CSMs) and 15 controls were included. Mean diffusion coefficient (ADC), fractional anisotropy (FA), and radial diffusivity (RD) were assessed in the visual pathways using DTI, and DTI values were compared between healthy subjects and patients before and after 12 months of GCR imaging. Additionally, the correlation between these values and radiosurgery data was also investigated.

Results: The ADC, FA, and RD values measured at visual pathways prior to and following GKR did not differ statistically. The FA values obtained from optic chiasm and occipital lobe were negatively correlated with the maximum and mean radiation dose to the prechiasmatic optic nerve and optic apparatus, respectively. The maximum radiation dose to the optic apparatus and the RD values obtained from the optic chiasm were found to be positively correlated. The maximum and mean radiation doses to the optic apparatus were found to positively correlate with the ADC and RD values obtained from the occipital lobe.

Conclusion: Defining the radiation-related microstructural diffusion changes in visual pathways following GKR may provide useful information for tailoring the radiosurgical approach and safety of the treatment. Diffusion tensor imaging may provide useful information to characterize changes of the radiation effects on visual pathways in patients with CSMs after GKR.

Keywords: Cavernous sinus meningioma, diffusion tensor imaging, magnetic resonance imaging, optic chiasm, visual pathways

INTRODUCTION

The prevalence of cavernous sinus meningiomas (CSMs) in the general population is 0.5 per 100 000.¹ The risk of meningiomas is increased by advanced age and female sex. Meningiomas are mostly benign, well-defined, and low-proliferating tumors.² It is possible to classify CSMs according to their anatomic localization. They may originate from the clinoid processes or dura of the cavernous sinus (CS), the sphenoid ridge dura, or the petroclival area that extends to or penetrates the CS.³ The most common presenting symptoms of meningiomas are ocular motor deficits, diplopia, ptosis, anisocoria, or complete ophthalmoplegia. The optic nerve compression by the tumor can cause visual field deficits, and carotid artery compression can cause ischemic deficits.⁴

CSMs usually cannot be completely resected because they are closely related to multiple critical structures, including the cerebral artery, optic nerves, ocular motor nerves, and pituitary body. Cavernous sinus meningiomas can be treated with systemic medicine, Gamma Knife Radiosurgery (GKR), surgical resection, attentive observation, or a combination of these various methods.^{2,3}

A magnetic resonance imaging (MRI) method called diffusion tensor imaging (DTI) is used to evaluate the microstructural changes in the white matter. The DTI evaluates visual pathways by measuring the changes in average diffusion coefficient (ADC), fractional anisotropy (FA), and radial diffusivity (RD) values of the visual pathways. Evaluation of FA provides information on the structural integrity of the fiber tracts, axonal degeneration, and structural irregularity while RD shows de/dysmyelination of white matter and changes in the axonal diameters or density.^{5,6} Previous DTI studies have found that reduced FA values are associated with visual impairment in a variety of diseases, such as Alzheimer's disease, moderate cognitive impairment, and glaucoma.⁷⁻²³

As far as the authors are aware, no research has been done in the literature to assess how radiation affects visual pathways in patients receiving GKR for meningiomas using the DTI approach. This study's objectives were to determine whether DTI altered visual pathways following GKR and to identify a connection between DTI and radiosurgery parameters in CSM patients.

MATERIAL AND METHODS

Thirteen patients (2 men, 11 women, median age 51 years; range: 31-81 years) with CSMs and 15 healthy controls (3 men, 12 women, median age 44 years; range: 32-57 years) were enrolled. Patients having conditions that can significantly affect DTI parameters, including as strokes, microhemorrhages, small-vessel disorders, and demyelination, were not included. 2 of patients had undergone operation because of CSM before GKR. The other patients treated by GKR first. The institutional ethics committee has accepted the study, which is a retrospective (decision dated March 13, 2018, numbered 6/70). The individuals who consented to participate in the study provided written informed consent. Radiosurgical variables including marginal dose, the mean and maximum dose receiving optic apparatus (including prechiasmatic segment of optic nerve and chiasm) were retrospectively reviewed. Then the doses received by the optic chiasm and prechiasmatic segment of optic nerve were calculated separately. Magnetic resonance imaging and DTI performed all cases before and 12 months after GKR. The ipsilateral and contralateral sides of the optic chiasm (Figure 1) and the subcortical white matter at the level of calcarine cortex in the occipital lobe (Figure 2) were used to measure the ADC, FA, and RD values. Average DTI values were found along the left side of the visual pathway in the control group. Computerized static perimetry performed to evaluate visual field before and 12 months after GKR. The MD (mean deviation), PSD (pattern SD) values were measured.

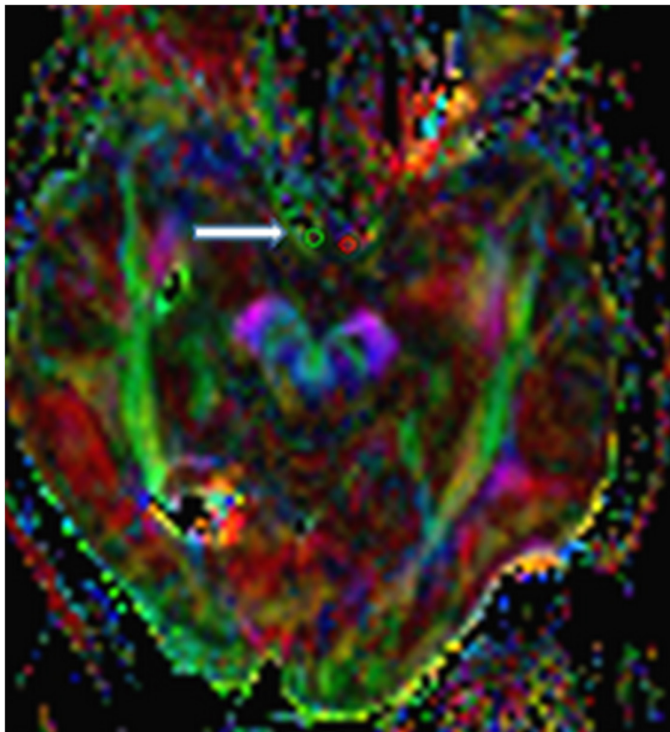


Figure 1. The axial color-coded maps shows the region of interests placed on the ipsilateral and contralateral optic chiasm (long arrow).

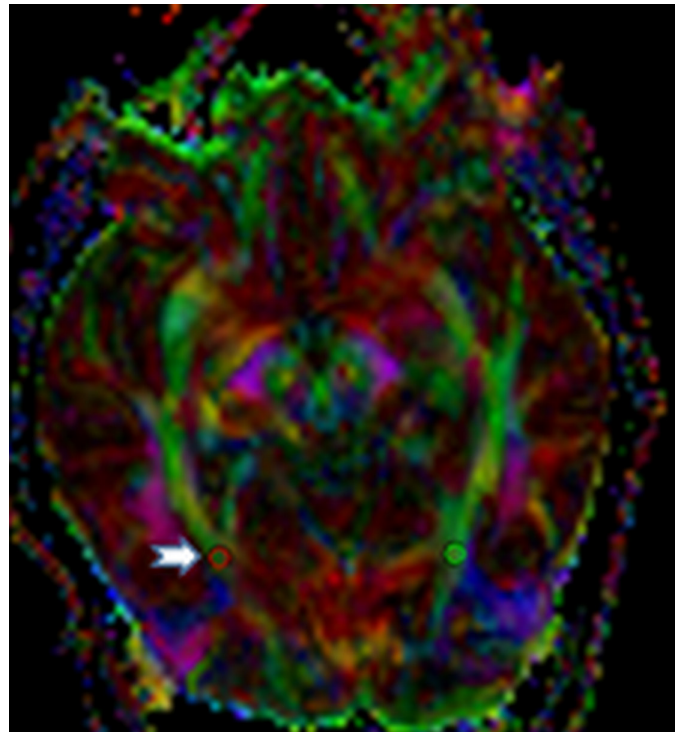


Figure 2. The axial color-coded maps shows the region of interests placed on the ipsilateral and contralateral occipital lobe (short arrow).

MRI Protocol: 1.5T MRI (Siemens, Avanto, Erlangen, Germany) was used with a head coil. T1-weighted (T1-W) spin echo (TR/TE, 460/14 ms), T1W with fat suppression (TR/TE, 715/7.5 ms) with and without contrast medium (gadolinium diethylenetriamine pentaacetic acid, 0.1 mmol/kg body weight, intravenously), T2-weighted (T2-W) turbo spin echo (TR/TE, 2500/80 ms), FLAIR (TR/TE, 8000/90 ms), T1-W spin echo (TR/TE, 460/14 ms) were obtained for brain MRI. With an isotropic voxel resolution of 1 mm, a magnetization-prepared rapid acquisition of gradient echo sequence was used to add the 3D T1-W volumetric sequences (TR/TE/TI, 12.5/5/450 ms) with and without contrast. An integrated parallel acquisition technique (iPAT) factor of 2 was used in conjunction with generalized autocalibrating partially parallel acquisition (GRAPPA) for parallel imaging. The DTI images obtained in the axial plane comprised a single-shot, spin echo, echo-planar sequence with TR/TE, 2700/89 ms; matrix, 128 × 128; field of view, 230 mm; slice thickness 5 mm; and 30 diffusion-encoding directions were used at $b = 1000 \text{ s/mm}^2$ and $b = 0 \text{ s/mm}^2$. Generalized autocalibrating partially parallel acquisition with an iPAT factor of 3 was used for parallel imaging. The Leonardo console (software version 2.0; Siemens) was used to rebuild the ADC, FA, and RD maps. The areas of interest (ROIs) were positioned and traced using the 3D T1-W and T2-W images as anatomical references. At the same section level, these images were combined with the matching area of the ADC and FA maps. At the level of the calcarine sulcus, each ROI was manually drawn with a size of 3 pixels at the chiasm and 4 pixels at the subcortical white matter of the occipital lobe. The ROIs' sizes and positions were adjusted by 2 experienced radiologists, who also evaluated them simultaneously on axial color-encoded FA maps based on "Dissecting the White Matter Tracts: An Interactive Instructional Atlas for Diffusion Tensor imaging." To avoid averaging artifacts and reduce the partial-volume effect, the slices above and below the region were compared side by side during ROI insertion

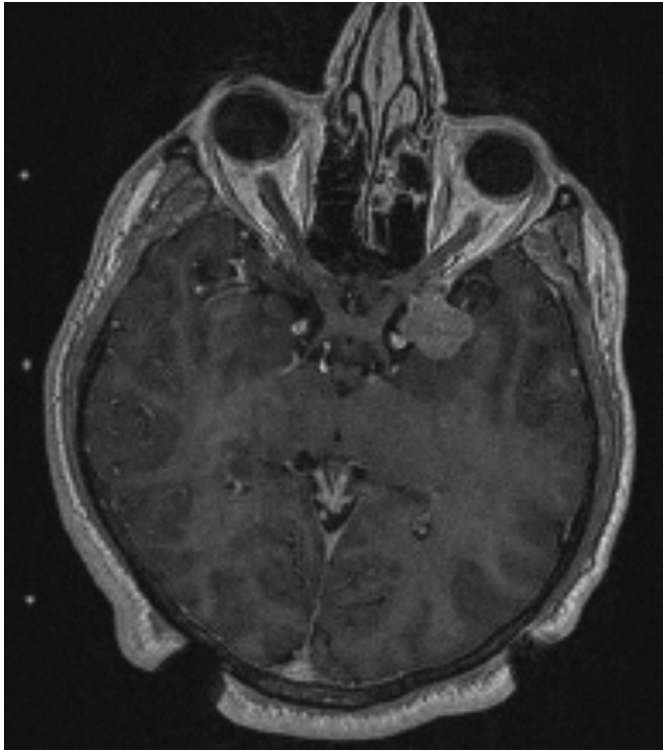


Figure 3. The axial 3D T1-weighted image, which used as an anatomic reference for treatment planning, shows the tumor and bilateral prechiasmatic parts of the optic nerves contoured to calculate the radiation dose received.

with the conventional images and color ADC, FA map, and diffusion trace.

Gamma Knife Protocol: The treatment was performed at the Gamma Knife Unit (Gamma Knife 4C model) of the university. After administering local anesthetic and placing a Leksell stereotactic head frame on the patient's head, MRI imaging was performed. The MRI data (T1W, T2W 3D images in the axial section) were transferred to the Gamma Plan version 10.1.1 software (Elekta AB, Stockholm, Sweden). The tumor and optic apparatus were contoured to plan treatment and perform dose calculations (Figure 3). The doses received by the optical apparatus were computed using the definition of the prescription dose. It is possible to modify the prescription dosage when certain factors surpass critical dose values. Every patient received a 50% isodose: the

median maximum optic apparatus dose was 8 Gy (range: 1-12 Gy) and median mean dose was 2.8 Gy (range: 1-5.7 Gy); the median treatment dose was 12 Gy (range: 10-14 Gy). No new neurological deficits were detected in any patients at 12 months after GKR.

Statistical Analysis

IBM SPSS 19.0 (IBM SPSS Corp.; Armonk, NY, USA) was used to analyze all of the data. ADC, FA, and RD values obtained from the visual pathways prior to and following GKR in the patients with CSMs and the control group were compared using ANOVA. To ascertain the connections among DTI results, radiosurgical treatment parameters, and visual field characteristics, the Tukey post hoc test was utilized. A type-1 error rate of $\alpha=0.05$ was used.

RESULTS

No statistical differences were observed in ADC, FA, and RD values measured from bilateral visual pathways prior to and following GKR in patients with CSM. There was no statistical difference in ADC, FA, and RD values measured in the control group and bilateral visual pathways before and after GKR in patients with CSM (Table 1).

The FA values obtained from optic chiasm were negatively correlated with the maximum and mean radiation dose to the prechiasmatic optic nerve (respectively, $r = -0.510$, $P = .011$, mean $r = -0.527$, $P = .008$). The maximum and mean radiation doses to the optic apparatus were negatively correlated with the FA measured from the occipital lobe (respectively, $r = -0.432$, $P = .035$, mean $r = -0.420$, $P = .04$).

The RD values obtained from optic chiasm were positively correlated with the maximum radiation dose to the prechiasmatic optic nerve and apparatus (respectively, $r = 0.429$, $P = .036$, $r = 0.406$, $P = .049$). There was a positive correlation between ADC and RD values measured from the occipital lobe and the mean radiation dose to the optic apparatus ($P < .05$).

Visual field tests and ophthalmological examinations were performed on all patients before and after GKR and in the control group. Patients with normal ophthalmological and fundus examinations and visual field tests were included in the control group. However, the results of 7 patients were obtained retrospectively. In these 7 patients, there was no statistical difference between MD and PSD values before and 12 months after GKR. There were no statistical differences between MD and PSD values before and 12 months after GKR, and there was no correlation between MD, PSA values, and DTI values (FA, ADC, RD)

Table 1. The Fractional Anisotropy, Average Diffusion Coefficient, and Radial Diffusivity Values Measured Before and After Gamma Knife Radiosurgery from Ipsilateral and Contralateral Sides in the Patients with Cavernous Sinus Meningioma and the Control Group

	Optic Chiasm			Occipital Lobe		
	FA	ADC	RD	FA	ADC	RD
Before GKR						
Ipsilateral side-before GKR	285 ± 89	1786 ± 547	1541 ± 532	331 ± 88	771 ± 74	644 ± 137
Contralateral side-before GKR	287 ± 117	1673 ± 314	1415 ± 314	361 ± 49	775 ± 78	653 ± 62
Control group	324 ± 97	1657 ± 480	1501 ± 540	339 ± 39	752 ± 53	613 ± 48
After GKR						
Ipsilateral side-after GKR	256 ± 65	2083 ± 802	1758 ± 582	319 ± 88	806 ± 102	666 ± 98
Contralateral side-after GKR	298 ± 44	1816 ± 470	1589 ± 671	326 ± 64	798 ± 105	653 ± 93
Control group	324 ± 97	1657 ± 480	1501 ± 540	339 ± 39	752 ± 53	613 ± 48
<i>P</i>	.35	.27	.57	.56	.45	.61

Data are presented as mean ± standard deviation ADC, apparent diffusion coefficient; FA, fractional anisotropy; RD, radial diffusivity; GKR, Gamma Knife radiosurgery. *P* values shows statistically not significant results

obtained at the optic chiasm and subcortical white matter of the occipital lobe obtained 12 months after GKR.

DISCUSSION

The optic strut separates the CS from the afferent visual pathway anteriorly, and the subarachnoid matter separates the optic nerve from the roof of the CS posteriorly. Nevertheless, the tumors that involve the CS can extend superiorly and affect the optic nerve or chiasm.²⁴ Recent studies have clearly indicated that curative surgery of CSMs alone is not a secure and sufficient treatment option in many cases. According to published research, surgery is linked to significant morbidity (17.9%–74%) and mortality (0%–9.5%) due to pituitary insufficiency, vascular damage, and cranial nerve abnormalities.^{25,26}

GKR is a reasonable, effective, and safe option for the primary or adjunctive treatment of these tumors. Radiosurgery has been widely used widely for treating benign tumors of the central nervous system. The most tumors that have been treated with GKR are acoustic neuromas and meningiomas of the skull base. It is important to preserve the neurological functions of the patients because meningiomas are benign lesions. Gamma Knife radiosurgery provides long-term overall tumor control and has extremely low morbidity rates.²⁷⁻²⁹ However, the optic apparatus is at risk of radiation toxicity.

Diffusion tensor imaging is a technique that determines the microstructural changes within the white matter by using diffusion measurements. Each DTI value (FA, ADC, and RD) is responsive to various aspects of white matter disease, such as neuronal damage, axonal degeneration, and maturation. Fractional anisotropy is very sensitive to changes in microstructure but less sensitive to changes of a particular kind (such as axial or RD). However, DTI is a potentially effective method for tracking how the brain reacts to treatments.⁵ Decreased FA and increased MD in the optic nerve are linked to progressive optic neuropathy, according to recent studies on glaucoma, amblyopia, retinitis pigmentosa, optic neuritis, and multiple sclerosis.¹⁵⁻²⁰ Nishioka et al²¹ reported that the visual pathway is impacted as Alzheimer's disease (AD) and moderate cognitive impairment (MCI) progress. In AD and MCI, there was an increase in RD and a decrease in FA at the optic nerve and tract. According to their findings, visual impairments in AD patients may be caused by damage to the visual white matter tracts. Adhikari et al²² stated that there was a negative correlation between retinotopically defined ganglion cell inner plexiform thickness (GCIPL) and optic tract MD and AD. The thickness of the retinotopically defined retinal nerve fiber layer was inversely connected with FA.

Chang et al²³ reported that significant relationships between Heidelberg Retina Tomography (HRT) rim area and DTI parameters in glaucoma patients. They showed that as HRT rim area decreased, MD, RD increased, while FA decreased in optic nerves. The retinal nerve fiber layer (RNFL) contains unmyelinated axons. Increased axonal loss in the RNFL is implied by a smaller retinal rim area. The linked downstream tissue, like the optic nerve, may experience myelin disintegration as a result of axonal degeneration, which also suggests axonal injury or loss.

For patients receiving radiosurgery treatment for CSM, GKR characteristics such as the mean and maximum radiation dose to the optical apparatus are crucial. According to the literature, CSMs are often treated for GKR with a peripheral dose of 12-14 Gy. To reduce the dose to organs at risk below 10 Gy, the tumor's closeness to optic pathways may dictate a dose reduction to 12 Gy.³ The volume of the optic

apparatus that receives large dosages is correlated with the likelihood of vision impairment. Klinger et al²⁸ showed that patients who received less than 10 Gy to the optic apparatus and those who received a peak dosage of less than 25 Gy to the CS did not experience any visual problems. In this study, the median maximum optic apparatus was 8 Gy (range: 1-12 Gy), the median optic apparatus dose was 2.8 (range: 1-5.7 Gy) and median treatment dose was 12 Gy (range: 10-14 Gy). There was no complication associated with visual pathways 12 months after GKR at the level of these radiation doses. It was found that ADC, FA, and RD values obtained from visual pathways do not significantly differ before and after GKR. Despite no statistical significance, there exists a trend for decrease in FA values in patients with CSMs before GKR compared to healthy controls.

Radiation therapy decreases the FA of impacted white matter regions, according to several research. The total radiation dose appears to have an impact on this decrease in FA, which might be used to evaluate dose distribution. While demyelination has no effect on the axial diffusivity, it may enhance the RD.⁵ The FAs recorded at the optic chiasm decrease as the mean and maximum radiation doses administered to the optic nerve rise. The RDs recorded at the optic chiasm increase in proportion to the maximal radiation exposure to the optic nerve and optic apparatus. As the maximum and mean radiation dose administered to the optic apparatus increase, the FAs obtained from the occipital lobe decrease and the ADC, RDs measured at the occipital dose increase. Decreased FA values in the occipital lobe and optic chiasma may indicate axonal structural irregularity, demyelination, axonal degeneration, and white matter disintegration. These findings in the study defining that the radiation dose-related microstructural changes in visual pathways following GKR. The limitation of this study is a small number of patients were included. And no other tests such as visual acuity or optical coherence tomography were performed on the patient or control groups. Fundus examination was not performed on the patient group. The fact that the visual impairments present in the patients before GKR treatment were not revealed by clinical data may have affected the findings in the comparison of DTI results of the control group and patients who underwent GKR.

To the best of the authors' knowledge, this is the first study to demonstrate DTI features of the visual pathways in CSMs patients treated with GKR. These results suggest that GKR does not change significantly the DTI changes at visual pathways. Microstructural diffusion changes in optic pathway were correlated with the mean and maximum radiation doses receiving optic apparatus at 12 months. Diffusion tensor imaging may provide useful information to characterize changes of the radiation effects on visual pathways in patients with CS meningioma after GKR.

Data Availability Statement: The data that support the findings of this study are available on request from the corresponding author.

Ethics Committee Approval: This study was approved by the Ethics Committee of Bezmialem Vakıf University (Approval No: 6/70; Date: 13.03.2018).

Informed Consent: Written informed consent was obtained from participants who agreed to take part in the study.

Peer-review: Externally peer-reviewed.

Author Contributions: Concept – H.O.T., A.A.; Design – A.A.; Supervision – A.A., M.H.S.; Resources – H.O.T., K.A., İ.Y.; Materials – K.A., İ.Y.; Data Collection and/or Processing – M.A.H., M.H.S., K.A., İ.Y., Ö.T.; Analysis and/or Interpretation – M.A.H., H.O.T., Ö.T.; Literature Search – H.O.T., İ.Y.; Writing Manuscript - H.O.T.; Critical Review – A.A., M.A.H.

Declaration of Interests: Alpay Alkan is an Emergency Radiology Editor at Current Research in MRI; however his involvement in the peer-review process was solely as an author. The other authors have no conflict of interest to declare.

Funding: The authors declared that this study has received no financial support.

REFERENCES

- Perry A, Scheithauer BW, Stafford SL, Lohse CM, Wollan PC. "Malignancy" in meningiomas: a clinicopathologic study of 116 patients, with grading implications. *Cancer*. 1999;85(9):2046-2056. (doi:10.1002/(sici)1097-0142(19990501)85:9<2046::aid-cnrc23>3.0.co;2-m)
- Correa SFM, Marta GN, Teixeira MJ. Neurosymptomatic cavernous sinus meningioma: a 15 years experience with fractionated stereotactic radiotherapy and radiosurgery. *Radiat Oncol*. 2014;9:1.
- Fariselli L, Biroli A, Signorelli A, Broggi M, Marchetti M, Biroli F. The cavernous sinus meningiomas' dilemma: surgery or stereotactic radiosurgery? *Rep Pract Oncol Radiother*. 2016;21(4):379-385. [CrossRef]
- Heth JA, Al-Mefty O. Cavernous sinus meningiomas. *Neurosurg Focus*. 2003;14(6):e3. [CrossRef]
- Alexander AL, Lee JE, Lazar M, Field AS. Diffusion tensor imaging of the brain. *Neurotherapeutics*. 2007;4(3):316-329. [CrossRef]
- Hui ES, Fu Q, So K, Wu EX. Diffusion tensor MR study of optic nerve degeneration in glaucoma. In: *Proceedings of the 29th Annual International Conference of the IEEE EMBS*. New York: IEEE; 2007:4312-4315. [CrossRef]
- Sidek S, Ramli N, Rahmat K, Ramli NM, Abdulrahman F, Tan LK. Glaucoma severity affects diffusion tensor imaging (DTI) parameters of the optic nerve and optic radiation. *Eur J Radiol*. 2014;83(8):1437-1441. [CrossRef]
- Garaci FG, Bolacchi F, Cerulli A, et al. Optic nerve and optic radiation neurodegeneration in patients with glaucoma: in vivo analysis with 3-T diffusion-tensor MR imaging. *Radiology*. 2009;252(2):496-501. [CrossRef]
- Engelhorn T, Haider S, Michelson G, Doerfler A. A new semi-quantitative approach for analysing 3 T diffusion tensor imaging of optic fibres and its clinical evaluation in glaucoma. *Acad Radiol*. 2010;17(10):1313-1316. [CrossRef]
- Engelhorn T, Michelson G, Waerntges S, Struffert T, Haider S, Doerfler A. Diffusion tensor imaging detects rarefaction of optic radiation in glaucoma patients. *Acad Radiol*. 2011;18(6):764-769. [CrossRef]
- Engelhorn T, Michelson G, Waerntges S, et al. A new approach to assess intracranial white matter abnormalities in glaucoma patients: changes of fractional anisotropy detected by 3 T diffusion tensor imaging. *Acad Radiol*. 2012;19(4):485-488. [CrossRef]
- Nucci C, Mancino R, Martucci A, et al. 3-T diffusion tensor imaging of the optic nerve in subjects with glaucoma: correlation with GDx-VCC, HRT-III and Stratus optical coherence tomography findings. *Br J Ophthalmol*. 2012;96(7):976-980. [CrossRef]
- Michelson G, Engelhorn T, Waerntges S, El Rafei A, Hornegger J, Doerfler A. DTI parameters of axonal integrity and demyelination of the optic radiation correlate with glaucoma indices. *Graefes Arch Clin Exp Ophthalmol*. 2013;251(1):243-253. [CrossRef]
- Chen Z, Lin F, Wang J, et al. Diffusion tensor magnetic resonance imaging reveals visual pathway damage that correlates with clinical severity in glaucoma. *Clin Exp Ophthalmol*. 2013;41(1):43-49. [CrossRef]
- Allen B, Schmitt MA, Kushner BJ, Rokers B. Retinothalamic white matter abnormalities in amblyopia. *Invest Ophthalmol Vis Sci*. 2018;59(2):921-929. [CrossRef]
- Zhang QJ, Wang D, Bai ZL, Ren BC, Li XH. Diffusion tensor imaging of optic nerve and optic radiation in primary chronic angle-closure glaucoma using 3T magnetic resonance imaging. *Int J Ophthalmol*. 2015;8(5):975-979. [CrossRef]
- Wang MY, Wu K, Xu JM, et al. Quantitative 3-T diffusion tensor imaging in detecting optic nerve degeneration in patients with glaucoma: association with retinal nerve fiber layer thickness and clinical severity. *Neuro-radiology*. 2013;55(4):493-498. [CrossRef]
- Li K, Lu C, Huang Y, Yuan L, Zeng D, Wu K. Alteration of Fractional anisotropy and Mean Diffusivity in glaucoma: novel results of a meta-analysis of diffusion tensor imaging studies. *PLoS One*. 2014;9(5):e97445. Published 2014 May 14. [CrossRef]
- Trip SA, Wheeler-Kingshott C, Jones SJ, et al. Optic nerve diffusion tensor imaging in optic neuritis. *Neuroimage*. 2006;30(2):498-505. [CrossRef]
- Samson RS, Kolappan M, Thomas DL, et al. Development of a high-resolution fat and CSF-suppressed optic nerve DTI protocol at 3T: application in multiple sclerosis. *Funct Neurol*. 2013;28(2):93-100. [CrossRef]
- Nishioka C, Poh C, Sun S-W. Diffusion tensor imaging reveals visual pathway damage in patients with mild cognitive impairment and Alzheimer's disease. *J Alzheimers Dis*. 2015;45(1):97-107. [CrossRef]
- Adhikari S, Qiao Y, Singer M, et al. Retinotopic degeneration of the retina and optic tracts in autosomal dominant Alzheimer's disease. *Alzheimers Dement*. 2023;19(11):5103-5113. [CrossRef]
- Chang ST, Xu J, Trinkaus K, et al. Optic nerve diffusion tensor imaging parameters and their correlation with optic disc topography and disease severity in adult glaucoma patients and controls. *J Glaucoma*. 2014;23(8):513-520. [CrossRef]
- Newman S. Prospective study of cavernous sinus surgery for meningiomas and resultant common ophthalmic complications. *Trans Am Ophthalmol Soc*. 2007;105:392-447.
- Skeie BS, Enger PQ, Skeie GO, Thorsen F, Pedersen PH. Gamma knife surgery of meningiomas involving the cavernous sinus: long-term follow-up of 100 patients. *Neurosurgery*. 2010;4:661-668.
- Sindou M, Wydh E, Jouanneau E, Nebbal M, Lieutaud T. Long-term follow-up of meningiomas of the cavernous sinus after surgical treatment alone. *J Neurosurg*. 2007;107(5):937-944. [CrossRef]
- Vera E, Iorgulescu JB, Raper DMS, et al. A review of stereotactic radiosurgery practice in the management of skull base meningiomas. *J Neurol Surg B Skull Base*. 2014;75(3):152-158. [CrossRef]
- Klinger DR, Flores BC, Lewis JJ, Barnett SL. The treatment of cavernous sinus meningiomas: evolution of a modern approach. *Neurosurg Focus*. 2013;35(6):E8. [CrossRef]
- Fatima N, Meola A, Pollom E, Chaudhary N, Soltys S, Chang SD. Stereotactic radiosurgery in large intracranial meningiomas: a systematic review. *World Neurosurg*. 2019;129:269-275. [CrossRef]